THE BEHAVIOUR OF A MUD-WATER INTERFACE UNDERNEATH A SLOWLY ADVANCING SHIP AT SMALL KEEL CLEARANCE

V. Ferdinande[1] and M. Vantorre[2]
State University Ghent - National Fund for Scientific Research
Grotesteenweg-Noord 2, B-9052 Zwijnaarde, Belgium

ABSTRACT

A mud layer on the sea bottom is simulated by a fluid layer of a certain thickness and density. A mixture of trichlorethane and petroleum seems to be the most appropriate fluid which can be used to simulate the water-mud interface.

Model experiments on a slowly advancing ship at small keel clearance revealed the existence of a hydraulic jump in the two-fluids interface, clearly pointing to a well-defined physical pattern. In order to explain, and to describe this phenomenon, that influences the resistance, sinkage, performance and, more important in practice, the manoeuvrability of the ship, some theoretical considerations are presented. It appears that a simplified approach, notwithstanding crude approximations, based on the continuity principle and on an application of Bernoulli's equation to the two-fluids layer problem, describes rather closely the main trends observed in the occurrence of the hydrodynamic phenomenon with varying parameters.

Even the occurrence of steering anomalies observed above muddy bottoms can be explained.

NOMENCLATURE

B : ship's beam
c : wave velocity
d : thickness of bottom layer
Fn : Froude number $U/\sqrt{gL}$
F_h : Froude number $U/\sqrt{gd}$
g : acceleration due to gravity
h : water depth
k : wave number $2\pi/\lambda$
K.C. : keel clearance
L : ship's length
m : blockage coefficient
N : yawing moment
p : pressure
Rn : Reynolds number UL/ν
S : ship's wetted cross section area
T : ship's draft
u : horizontal velocity in fluid layer
U : ship's speed
V : fluid velocity
w : tank width, or, vertical component of V
x : distance of zero-crossing interface jump to FP, or, horizontal distance in general
Y : hydrodynamic lateral force
z : vertical distance in general
δ : boundary layer thickness, or rudder angle
ζ : interface rise (pos. or neg.)
λ : wave length (interfacial)
μ : dynamic viscosity coefficient
ν : kinematic viscosity coefficient
ρ : mass density
ω : circular frequency

subscripts
1 : pertaining to upper (water) layer
2 : pertaining to lower (mud) layer
a : pertaining to layer part behind the jump (aft side)
b : pertaining to layer part before the jump (bow side)

superscripts
' : indicates non-dimensional
* : fictive value, or, relative to the ground
(c) : critical value

INTRODUCTION

Ship-owners and harbour authorities show an increasing interest in the safe steering and manoeuvring at low speed of large vessels at very small keel clearance above a muddy bottom. The study of the hydrodynamic phenomena occurring in such circumstances has become a necessity. However, scientific investigation of mud layers, and of the fluid flows above and in them, apparently is a difficult task, [1], [2], [3], [4], [5]. An engineer's approach looks rather risky, because inevitably based on bold hypotheses in order to make the study more feasible. Nevertheless, it appears to be justified to regard the real natural situation as a two-layer fluid problem. The mud layer on the hard bottom is represented by a fluid layer of a certain density (higher than that of water) and a certain thickness, separated from the water by an interface, through which no mixing of the two fluids can occur. Some years ago, R. Sellmeyer and G. van Oortmerssen [6] introduced this experimental technique, and carried out model experiments on a manoeuvring tanker above a bottom layer of a chlorinated paraffin and kerosine mixture, that should simulate the real mud layer.

In the present paper, the relative ship speeds (or Froude numbers) considered are lower yet than in [6], rather corresponding to those when approaching a berth or a lock, and this paper deals mainly with the undulation of that interface while the ship is

1. Professor, M.S., director
2. Research Associate, Ph. D.

advancing above, or through it, at those very low speeds. The observed phenomenon, viz. the jump in the interface, is different in character from the internal waves as observed in and pointed to in [6], (at higher ship's speed).

The influence of a mud layer on ship resistance, powering performance, and especially squat and trim, and manoeuvring, at the usual low speeds, will be discussed in more details, and in a more rigorous mathematical way, by the second author in a following paper.

NAVIGATION IN MUDDY AREAS

In some areas the bottom conditions of the sea and estuaries are characterized by the presence of a muddy bed.

Some work achieved in the field of mud layer study, as far as navigation is concerned, is acknowledged here by referring to [7], [8], [9]. Attention also has to be drawn to the results of a study project on optimization of maintenance dredging works organized by the Belgian Coastal Service, [10], [11]. It attempts to determine the navigable depth for safe manoeuvring. However, this "nautical depth", and required minimum keel clearance as well, is difficult to assess. An upper part of the mud layer has such low density and small shear strength, that a "nautical bottom" can be defined, lying at a certain distance under the mud-water interface (which can be detected by echo-sounding surveys with 210 kHz accoustic frequency), and under which the density and rigidity increase rather abruptly with depth, becoming too dense and too rigid to behave as a fluid. This nautical bottom as defined is thought to be detected by echo-sounding at 33 kHz, [12], [13], [14]. Defining the nautical bottom depends on a proper choice of density, and on the deformation behaviour of the mud deposit and its shear strength, which depends on the rheological properties (initial rigidity and dynamic viscosity) of that mud, [9], [10], [12], [13], [14]. For example, densities for a definition of the nautical bottom in Zeebrugge, appear to be in a range of 1.15 to 1.26 ton/m^3, depending on the sand content of the mud.

The resistance and manoeuvrability characteristics of a ship sailing at small, or even negative bottom keel clearance with respect to the interface water-mud are influenced by the mud bottom layer in some way.

The existence of a certain undulation pattern in the mud-water interface has been known for several years, [6], [7], [8], and has been confirmed by full-scale investigations on a suction hopper dredger under sail at small keel clearance (Zeebrugge, 1986), [9], [10].

MODEL EXPERIMENTS

During tank experiments on ship models, an undulation pattern similar to that observed during full-scale investigations could be created in the interface between the water and several liquids of higher density, such as natural mud, artificially composed mud and a mixture of trichlorethane and petroleum (TCE/P), the density of the latter depending on the ratio. This TCE/P was selected as mud-simulating material for some series of systematic experiments carried out on two self-propelled ship models. The hypothesis that a layer of a certain thickness of this liquid may simulate the mud layer as present on the site of the full-scale measurements appeared to be valid in many respects.

A schematic general picture of the longitudinal profile of the undulated interface alongside the ship is shown in Fig.1, in order to point to a special feature, namely the intersection 0 of the disturbed interface with the original interface line at rest. This upward zero-crossing, as it could be called, when going from the FP to the AP, is characterized by the relation x/L. Of course, this picture in Fig.1 is merely schematic. The profile of the "sunken" interface between 0 and FP is not evenly horizontal, nor is the "risen" interface aft of 0, which moreover shows some secondary undulations when 0 is not too near AP, (see Fig.11). Visual observations let state that the crests of these undulations alongside the ship are perpendicular to the longitudinal axis, extending to the tank walls. The term "undulation" of the interface is used here intentionally, instead of "internal wave", because the main zero-crossing phenomenon corresponds in no way with the known behaviour of internal waves (e.g. regarding velocity). The sudden change of interface level around 0, from negative to positive, rather suggests a "hydraulic jump" phenomenon. It must be emphasized, however, that all ship's speeds considered here are relatively very low (Fn $\leq$ 0.06). For higher speeds, the "jump" is situated behind the stern, and the angle between the crests and the centerline decreases.

In a shallow water tank of width w = 2.25 m, two different self-propelled ship models have been used in the experimental study of the interfaces, one called DRAGO (1/40 scale model of the suction dredger "Vlaanderen XVIII"), the other called METO (1/70 scale model of a LNG-carrier). Relevant characteristics of the models are

	DRAGO	METO
L(m)	2.888	3.81
B(m)	0.575	0.59
T(m)	0.200	0.16
C_B	0.84	0.80

During the runs above the TCE/P layer, the vertical position of the TCE/P-water interface was recorded at one single location in the tank by means of a "bottom profile tracker".

Model tests were carried out over a speed range U (of low Fn) at a given draft T of the model. Different bottom keel clearances (with respect to the interface), K.C. = 100 (h/T-1) in per cent, were obtained by changing the water depth h. Other parameters are the thickness of the TCE/P-layer d and its density ρ_2. The dynamic viscosity of the lower fluid layer had a practically constant value of 0.002 Pa.s.

The parameters for the different experimental test series were :

DRAGO : T = 0.20 m
- d = 0.035 m , ρ_2 = 1,220 kg/m^3 and 1,110 kg/m^3
  K.C. = 20 , 10 , 4 , 2 , 0 , -2 , -4 per cent of T
- d = 0.016 m , ρ_2 = 1,110 kg/m^3
  K.C. = 10 , 4 , 0 , -4 per cent of T

METO : T = 0.16 m
- d = 0.011 m , ρ_2 = 1,140 kg/m^3
  K.C. = 10 , 4 , 2 , 0 , -2 per cent of T

At a given forward ship speed, variations in K.C. alter x/L but very slightly, in contrast with the important influence on x/L of varying ρ_2, and varying d, or both.

Fig.2 shows the measured values of x/L in the tank, versus Froude number Fn = U/$\sqrt{gL}$. No distinction is made here between different keel clearances in plotting the dot characters per ship, distinction being made only for density ρ_2 and thickness d of the bottom layer.

It is remarkable how all dots pertaining to each case fall in distinct narrow bands, particularly in a range x/L < 1.

Generally, when experimental values concerning a certain physical phenomenon all fall "on one line", with little scattering, viz. with very small standard deviation, one may not only presume that the experimental procedure is sufficiently accurate, but also that this points to the existence of a well-defined physical pattern. Such "experimental line" should be taken as a base for guidance of any theoretical elaboration to explain the phenomenon, and to calculate data concerned. Any systematic and distinct divergence from this experimental line should be regarded as an indication of erroneous theoretical treatment, or of a non-consideration of one or more physical facts, that actually do play an important role in the phenomenon, in some particular circumstances at least. Satis

factory agreement of the theoretical results with a trustworthy experimental line may inspire confidence in that theoretical approach, even if it may look very simplistic. On the other hand, any appreciable deviation, found in some range of the governing parameters, should prompt the author of the theory to find an adequate refinement, to look for another approach, or to involve other physical factors, not taken into account in his previous work.

The results of the actual experiments under various conditions show clearly the existence of some trends, which can be described as follows :

- 0 moves aft with increasing ship speed U,
- at the same U, 0 shifts backwards with decreasing density ρ_2 of the bottom fluid layer,
- at the same U and ρ_2 , 0 shifts backwards with decreasing thickness d of the bottom layer.

It also appears that a difference in keel clearance, e.g. from 20 to -4 per cent, does not alter the ratio x/L in a significant way.

A SIMPLIFIED THEORY

A theoretical treatment of some physical events as described in the introduction has been presented already before, [15]. A simplified theory is given below. Its role is thought to explain more easily the trends revealed by the experiments, rather than rendering trustworthy quantitative results (although the latter seemed to be quite valuable after all).

As said before, it is quite remarkable that the measured values of x/L during the numerous runs executed at different (low) speeds, for the two ship models in distinct conditions regarding ρ_2 and d, show but very little dispersion. Insomuch that these experimental results should be regarded as a strong basis for validation of any theoretical inference about these flow phenomena. Were the inferred ratio x/L different from what is observed to be, then a reason for the discrepancy ought to be sought, and explained.

Account has been taken of the fact that the heights of level variations of the free water surface are only a small fraction $\Delta\rho/\rho_2$ (with $\Delta\rho = \rho_2-\rho_1$) of those of the lower interface, in that the former simply have been neglected here. We merely place emphasis upon the bottom layer TCE/P, with density ρ_2, a little higher than $\rho_1 = 1$ of the water, so $\Delta\rho/\rho_2$ being very small indeed.

The cross section of the tank in Fig.3 refers to one section fore and one section aft of the FP. Because keel-clearance variations apparently have but very little effect on the phenomena described here, no sinkage of the ship model is taken into account in the following computations.

With the symbols and axes as declared in Fig.3, and making no account of viscosity, Castelli's rule is written as

$$wdU = -[w(d + \zeta)]u_2 \qquad (1)$$

in fluid 2, viz. the TCE/P layer,

$$whU = -[w(h - \zeta) - S_1]u_1 \qquad (2)$$

in fluid 1, viz. the water.

Applying Bernoulli's equation along the interface, but consecutively on both sides, thus in fluid 1 and fluid 2, and assuming the continuity of pressure across the interface, following relation is derived (see Appendix),

$$\rho_2\left(\frac{1}{2}u_2^2 + g\zeta\right) - \rho_1\left(\frac{1}{2}u_1^2 + g\zeta\right) = \frac{1}{2}(\rho_2 - \rho_1)U^2 \qquad (3)$$

Dimensionless presentation of these relations :

$$u_2' = -\frac{1}{1 + \zeta'} \quad , \quad \text{or } \zeta' = -(1 + \frac{1}{u_2'}) \qquad (1')$$

$$u_1' = -\frac{1}{1 - m_1 - d'\zeta'} \qquad (2')$$

$$\rho_2' u_2'^2 - \rho_1' u_1'^2 + 2\frac{\zeta'}{F_2^2} = 1 \qquad (3')$$

where

$$u_1' = \frac{u_1}{U} \quad , \quad u_2' = \frac{u_2}{U} \quad , \quad \zeta' = \frac{\zeta}{d} \quad , \quad d' = \frac{d}{h}$$

$$\rho_1' = \frac{\rho_1}{\rho_2 - \rho_1} \quad , \quad \rho_2' = \frac{\rho_2}{\rho_2 - \rho_1}$$

$$m_1 = \frac{S_1}{wh} \quad , \quad F_2 = \frac{U}{\sqrt{gd}}$$

m_1 = a blockage coefficient,
F_2 = a Froude number based on bottom layer thickness.

Substituting u_1' and u_2' in (3') leads to

$$F = \frac{\rho_2'}{(1 + \zeta')^2} - \frac{\rho_1'}{(1 - \zeta' d' - m_1)^2} + 2\frac{\zeta'}{F_2^2} - 1 = 0 \qquad (4)$$

Characteristic curves representing the function F for different values of F_2 at given ρ_1', ρ_2' , d' and m_1 , are sketched in Fig.4. The possible values of ζ', viz. roots of equation (4), are $-1 < \zeta_b' < 0$, and $\zeta_a' > 0$. For some small F_2, two real values of ζ' are found between 0 and $(1-m_1)/d'$; for greater values of F_2, those roots are imaginary ; for a certain value $F_2^{(0)}$, to be determined, the first positive roots ζ_a' are equal, and exceeding the corresponding critical ship speed results in a sudden jump to a much higher $\zeta_a' > (1-m_1)/d'$.

The existence of different roots can be interpreted as the possibility of (at least) two different pictures of flow in the two-fluids layer of Fig.3. ζ_b' (subscript refers to bow) suites the part of ship length bow side, inception being the (small) positive pressure at the bow associated with the potential flow actually present. This value is always negative, i.e. the TCP/water interface has sunk. The principle of mass conservation in the bottom layer requires that at a certain distance from the bow, this interface must rise again to compensate. This rise above the initial, undisturbed interface level equals the first positive ζ_a' (subscript : aft).

For the different cases considered here, the values of ζ_b' and ζ_a' are plotted versus F_2 and Fn in the Fig. 5a, b, c, d, in which also the corresponding values according to (1') and (2') of u_{2b}' , u_{2a}', u_{1b}' , u_{1a}', respectively are shown. If, for the sake of simplicity, this difference in interface level between zones a and b is restricted to an area of constant width between the ship's perpendiculars, then, because of the continuity principle, the longitudinal position of the jump in the interface should be given by

$$\frac{x}{L} = \frac{\zeta_a'}{\zeta_a' + |\zeta_b'|} \qquad (5)$$

These theoretical values of x/L are plotted versus Fn in Fig.6. The relation between the Froude number and F_2 is

$$Fn = \sqrt{\frac{d}{L}}\,F_2 \qquad (6)$$

The choice of the dimensionless number F_2 followed automatically from (3) after having chosen the dimensionless velocities as $u_1' = u_1/U$ and $u_2' = u_2/U$ and the dimensionless interface rise (positive and negative) as $\zeta' = \zeta/d$. Actually, F_2 cannot be considered as a very speaking measure of ship speed, but its advantage is in that d has but a secondary effect in (4). Hence, merely altering the

bottom layer thickness d at a given F_2, doesn't influence significantly the value of ζ', in particular ζ'_b.

The theoretical and the experimental results x/L are matched, per combination of ρ_2 and d, and for the different values of K.C., in Fig. 7a, b, c, d.

One can see in Fig.2, that for higher Fn , x/L > 1, viz. the jump is located somewhere behind the stern. Of course, such a value of x/L cannot be obtained by the simple theoretical procedure presented here, but the sudden immense increase of ζ'_a when exceeding $F_2^{(0)}$, viz. a critical ship speed, let us surmise that in reality the jump shifts more backwards.

However, with d = 0.035 m for DRAGO, the agreement in Fig. 7a, b is quite good over an important range of Fn, except at the lowest ship speeds, where the measured x/L are lower than the theoretical values. In this latter case, one can observe on records of the longitudinal interface profile, that the area between initial and sunken interface is significantly smaller than between initial and risen interface behind the jump, as contrasted with the assumption on which (5) is based. The width over which the sinkage of the interface extends along the foreship may be larger than the width of the rise behind the jump, because of fluid pressure associated with the potential flow at the bow. The divergence for x/L < 0.5 is also partly due to smaller, diminishing cross section areas towards the FP, corresponding to a fictive lower blockage.

A more serious deviation is remarked when the thickness of the bottom layer is really very small, (Fig. 7c, d). The experimental mean curve indicates much lower x/L-values over the whole range of Fn. In this case viscosity seems to play an important role in the sublayer b (near the bow).

As $|u'_{2b}| > 1$, $|u_{2b}|$ is larger than U, the latter being also the horizontal velocity of the hard bottom relative to the ship. Hence, a boundary layer, which is laminar at those low Reynolds numbers in the tank, with increasing thickness δ from the fore entrance to the jump, is existing in the bottom layer b, with thickness $d-|\zeta_b|$, (Fig.8).

For a given ship speed U, in non-viscous fluid the velocity u_{2b} should be uniform over the height $d-|\zeta_b|$ for the x/L having the value as calculated above. This is not so for reasons of viscosity : the fluid velocity u in fact is as indicated by the hatched surface (A) in Fig.8

$$u = U + \left(\frac{2}{\delta} y - \frac{1}{\delta^2} y^2\right)(2 u_{2b} - U) \tag{7}$$

(here u_{2b} and ζ_b are absolute values).

The boundary layer thickness δ for laminar flow in our case is given by

$$\delta = 4.9 \sqrt{\frac{\nu x}{u_{2b} - U}} \tag{8}$$

($\nu = 1.8 \times 10^{-6}$ m²/s for $\rho_2 = 1{,}220$ and 1.6×10^{-6} m²/s for $\rho_2 = 1{,}110$ kg/m³)
and presented in Fig.9 for METO and DRAGO.

The mean value $\overline{u}_{2b}$ over $d-\zeta_b$, but made dimensionless, is

$$\overline{u}'_{2b} = 1 + \frac{d}{\delta}\left(1-\zeta'_b\right)\left(u'_{2b}-1\right) - \frac{d^2}{3\delta^2}\left(1-\zeta'^2_b\right)\left(u'_{2b}-1\right) + \left|\left(1-\frac{\delta}{d(1-\zeta'_2)}\right)u'_{2b}\right| \tag{9}$$

(the last term in brackets to be included when $d-\zeta_b > \delta$).

In the cases of thin bottom layers (METO : d = 0.011 m ; DRAGO : d = 0.016 m), $\overline{u}'_{2b}$ is much smaller than the calculated u'_{2b} in inviscid fluid, and a value of x/L calculated as such cannot be expected to be true. In fact, u'_{2b} should be taken much larger, in order to arrive at a $\overline{u}'_{2b}$ that equals the first mentioned u'^{*}_{2b}. Hence, for a given U, we should adopt u'^{**}_{2b} that results in $\overline{u}'^{**}_{2b} = u'^{*}_{2b}$. This u'^{**}_{2b} is

$$u'^{**}_{2b} = 1 + \frac{u'_{2b} - 1 - \left|1 - \frac{\delta}{d} u'_{2b}\right|}{\frac{d}{\delta}\frac{1}{u'_{2b}} - \frac{d^2}{3\delta^2}\frac{1}{u'^2_{2b}} + \left|1 - \frac{\delta}{d} u'_{2b}\right|} \tag{10}$$

(terms in brackets to be included when $d - \zeta_b > \delta$)

The values u'^{**}_{2b} can be quite large, corresponding in Fig.5 with a low F_2 noted F_2^* . For equal ship speed, thus for the same Fn ,

$$F_2 = \sqrt{\frac{d^*}{d}}\, F_2^* \tag{11}$$

while for equal values of F_2^*, as commented earlier, the values of ζ'_b are but little affected by the value of d, or d^*. Hence, for F_2^*, ζ'^{**}_b can be read from Fig.5, and is seen to be larger in absolute value than the ζ'_{2b} found first. Keeping ζ'_a unchanged (in the bottom layer on side a, the flow behaves in another way, with velocities reversed with respect to the fixed bottom), we see that $x/L = \zeta'_a/(\zeta'_a + |\zeta'^{**}_b|)$ is smaller, and the results are closer to the experimental curve in Fig.7c,d.

The same procedure applied to the cases with d = 0.035 m lowers the theoretical curve x/L in Fig.7 a,b but only slightly. Hence, the simplified approach may be used for not too small a d, e.g. minimum 0.03 m.

If along the interface $\partial\zeta'/\partial x$ takes a large value, then (A.9) of the Appendix should be used, where, in our case,

$$u_2 = -\frac{U}{1 + \zeta/d} \quad \text{and} \quad u_1 = -\frac{U}{1 - m_1 - \zeta/h}$$

Adopting the non-dimensional notations x' = x/L and h' = h/L, (A.9) can be written as

$$F' = \frac{\rho'_2}{(1+\zeta')^2} - \frac{\rho'_1}{(1-m'+d'\zeta')^2} + 2\frac{\zeta'}{F_2^2} - 1 + \left|\frac{\rho'_2}{(1+\zeta')^2} - \frac{\rho'_1}{(1-m'+d'\zeta')^2}\right| d'^2 h'^2 \left(\frac{\partial\zeta'}{\partial x'}\right)^2 - 2\left|\rho'_1 Rn_1^{-1}\frac{d'}{(1-m_1-d'\zeta')^2} + \rho'_2 Rn_2^{-1}\frac{1}{(1+\zeta')^2}\right|\frac{\partial\zeta'}{\partial x'} = 0 \tag{12}$$

where Rn is the Reynolds number UL/ν respectively for fluid 1 and fluid 2, and $\partial\zeta'/\partial x'$ is the non-dimensional slope = L/d times (slope of the interface).

INTERFACIAL WAVES

If the thickness d of the bottom fluid layer is small, compared to wave length and the water depth h, the velocity of an internal wave is

$$c_{max} = \sqrt{\frac{\Delta\rho}{\rho_2} g d} \tag{13}$$

which is the maximum velocity for this thickness d.

The value of (13) is different from the ship speeds developed during the runs in the tank. Ship speeds higher than c_{max} are reached, the hydraulic jump being located yet between the ship's perpendiculars. This is in particular so if d is small, but the critical ship speed approaches c_{max} for DRAGO 20% K.C., d = 0.035 m. Table I shows these values as calculated.
The hydraulic jump as described is not an interfacial wave.

At the hydraulic jump, the interface shows a slope, of course. Hence, formula (12) should be used. It results in a larger ζ'_a and a smaller absolute value of ζ'_b, compared with these respec-

Table I

	d (m)	ρ_2 (kg/m³)	K.C (%)	$U_{critical}$ (m/s)	C_{max} (m/s)
METO	0.011	1140	10	0.17	0.115
	0.011	1140	0	0.16	0.115
DRAGO	0.035	1220	20	0.27	0.250
	0.035	1220	0	0.22	0.250
DRAGO	0.035	1110	20	0.19	0.185
	0.035	1110	0	0.16	0.185
DRAGO	0.016	1110	20	0.19	0.125
	0.016	1110	0	0.16	0.125

tive values found in the case of zero interface slope. For example, DRAGO, ρ_2 = 1,110 kg/m³ , d = 0.035 m, K.C. 20%. F_2 = 0.22 (U = 0.129 m/s)

slope $\partial\zeta/\partial x$	=	0	1/4	1/2	1
ζ_a'	=	0.28	0.29	0.375	0.92
ζ_b'	=	-0.48	-0.415	-0.375	-0.28

This means that the jump must show something like an overshoot in its upper part. The latter could be considered as a disturbance, giving rise to a pattern of transversal interfacial waves behind the jump. This progressive interfacial wave should have a velocity in accordance with the relation given by Wehausen and Laitone in [16], if the two fluids were assumed to be initially at rest :

$$\left(\frac{\omega^2}{gk}\right)^2 (\rho_2 \coth kh_a \coth kd_a + \rho_1) - \frac{\omega^2}{gk}\rho_2 (\coth kh_a + \coth kd_a) + (\rho_2 - \rho_1) = 0 \qquad (14)$$

which gives two possible solutions for ω^2 for a given wave number k. Here, h_a and d_a are the thicknesses of the upper layer and the lower layer respectively behind the jump. In our case, $\coth kh_a \approx 1$, and the equation (14) has the solutions $\omega^2 = gk$ and

$$\omega^2 = gk \frac{\rho_2 - \rho_1}{\rho_2 \coth kd + \rho_1} \qquad (15)$$

the latter being the smallest solution, which we retain. A graph of ω^2/gk versus kd is given in Fig.10 for ρ_2 = 1.11 (DRAGO) and ρ_2 = 1.14 (METO). For several ship speeds in the case DRAGO, ρ_2 = 1.110, d = 0.035 and for METO, ρ_2 = 1.14 and d = 0.011, the interface profiles are shown in Fig.11 (with different scales in vertical and longitudinal direction). The (average) wave lengths λ of the progressing interfacial waves can be measured on them.

However, it should be remarked that the two fluids have their own horizontal velocities u_{1a} and u_{2a} (Fig.5). Hence, the waves are expected to be deformed, and travelling in media of which the speed is a mean of u_{1a} and u_{2a}.

Some relevant figures are given in the Table II.
The calculations give a value c* somewhat lower than U. We dare not draw any conclusion from this, however, because the real flow in the layers b seems to be more complex than assumed in the present simplified view. In any case it is clear that the velocity of these interfacial waves is lower than the maximum value

$$c_{max} = \sqrt{\frac{\rho_2 - \rho_1}{\rho_2} g (d + \zeta_a')} \qquad (16)$$

that could be reached in layer 2a, as indicated in the last column of Table II.

Table II

U (m/s)	λ (m)	$\bar{u}$ (m/s)	d_a (m)	ω (rad/s)	c (m/s)	c* (m/s)	c_{max} (m/s)
Drago ρ_2 = 1.110 d = 0.035 K.C. 20 %							
0.136	0.255	0.141	0.0455	3.35	0.135	0.131	0.210
0.153	0.300	0.157	0.0525	3.07	0.147	0.143	0.226
0.169	0.325	0.174	0.0595	2.98	0.153	0.149	0.240
0.178	0.325	0.180	0.0655	3.07	0.153	0.152	0.252
0.183	0.335	0.186	0.0700	2.97	0.159	0.156	0.261
Meto. ρ_2 = 1.140 d = 0.011 K.C. 10 %							
0.123	0.16	0.123	0.020	4.41	0.112	0.112	0.159
0.131	0.18	0.126	0.023	4.18	0.120	0.125	0.166
0.175	0.29	0.189	0.055	3.54	0.163	0.150	0.257

($\bar{u} = \frac{u_{1a}' + u_{2a}'}{2} \cdot U$, c* with respect to the ground)

In the formulas (A.4), (A.8), (A.9) of the Appendix, and (12), viscosity is taken into account. However, the current values of ν of the mud simulating fluid as used here is less than twice that of water, and its influence on the results appears to be negligible. Even in the case of a fluid with viscosity 25 times that of water, as used in [6] , no significant influence can be noticed. A comparison is given below for the case DRAGO, ρ_2 = 1,100, d=0.035, K.C. = 20%, F_2 = 0.22 (U = 0.129 m/s) ;

slope	1/4		1/2		1	
	(1)	(2)	(1)	(2)	(1)	(2)
ζ_a'	0.29	0.29	0.375	0.38	0.92	0.93
ζ_b'	-0.415	-0.42	-0.375	-0.38	-0.28	-0.29

(1) : ν = 1.8 x 10⁻⁶ m²/s , (2) : ν = 25 x 10⁻⁶ m²/s

POSSIBLE STEERING ANOMALIES

According to a recent survey report, one day, a bulk carrier proceeding towards the entrance of a lock at dead slow ahead with rudder amidships, started veering to the port side and hit the lock entrance wall. No clear reasons could be found by the nautical experts. However, keel clearance appeared to be about 20%, but it is well known the bottom in this area is covered by a mud layer. Maybe the reason of an "instability" in steering could be sought in the presence of that mud layer.

During several experiments in the tank, viz. on the DRAGO model, lateral forces and yawing moments have been measured. These are thought to be induced by the global rudder action at a given rudder angle, and are presented as dimensionless

$$Y' = \frac{Y}{1/2\,\rho_1 L^2 U^2} \qquad N' = \frac{N}{1/2\,\rho_1 L^3 U^2}$$

Without a "mud" layer, the trend of Y' and N' is normal for all values of K.C., as schematically indicated in Fig.12. However, with a TCE/P bottom layer, anomalies appeared in certain circumstances, e.g. Drago, ρ_2 = 1110 kg/m³ , d = 0.035 m, K.C. 0 % (Fig.12), where for $\delta = 0°$, N' was significantly negative and about 0 at $\delta = 10°$, while Y' showed a negative value at $\delta = 10°$, where normally it should be positive. Closer investigation made it clear that those instabilities in rudder action occurred when the risen interface came into touch with the aft ship hull. This happened mainly at keel clearances around 0 % (positive and negative), and in a rather restricted range of ship speeds near the critical speed. At K.C. = 20 %, no significant anomalies could be noticed yet. In order to determine the exact circumstances in which contact of the risen part of the interface with the ship bottom occurs, squat and trim should be determined as well. For

this, more rigorous calculations should be executed, taking due account of the free water surface, which was assumed to be unchanged so far. This is done in a paper to be presented by the second author.

As the physical phenomena in the sublayer behave as though the gravitational action is reduced to $g' = (\Delta\rho/\rho_2)g$, a pressure difference on both sides of the hull that is immersed in the risen aft bottom layer can provoke a significant difference in the level of the interface at port and starboard side. A transversal force, and an associated yawing moment can result. The pressure difference on port and starboard side can result from moderate rudder angle, from screw action, or from any unsymmetrical pressure disturbance caused by some event in the environment.

ACKNOWLEDGEMENTS

This study of the behaviour of mud layers and of ships moving above them is organized by the Coastal Service, Ostend, of the Flemish Administration of Waterways and Maritime Affairs. The model test program is carried out at the Hydraulic Research Laboratory, Antwerp-Borgerhout, of the same Administration, scientifically supported by the Dienst voor Scheepsbouwkunde (Office of Naval Architecture) of the State University Ghent and the Belgian National Fund for Scientific Research. Full-scale navigation tests were executed by a joint venture of Baggerwerken Decloedt & Zoon NV, Dredging International N.V., Jan De Nul N.V. and Haecon N.V.

REFERENCES

1. Migniot,C., Etude des propriétés physiques de différents sédiments très fins et de leur comportement sous des actions hydrodynamiques, *La Houille Blanche*, No 7, 1968, pp. 591-620.
2. Migniot,C., Les matières en suspension dans les estuaires. Bull. Association International de Géologie de l'Ingénieur, No 28, Paris 1983, pp. 61-75.
3. Migniot,C., Tassement et rhéologie des vases, La Houille Blanche, No 1, 1989, pp. 11-29.
4. Verreet,G., Van Goethem,J., Viaene,W., Berlamont,J., Houthuys, R., Berleur, E., Relations between physico-chemical and rheological properties of fine-grained muds, 3rd Int.Symp. on River Sedimentation, Jackson, 1986, pp.1637-1646.
5. Mei,C.C., Liu,K.F., A Bingham-plastic model for a muddy seabed under long waves, Journal of Geophysical Research, Vol.92, No C 13, December 1987,pp. 14,581.
6. Sellmeijer,R., van Oortmerssen,G., The effect of mud on tanker manoeuvres, RINA 1983.
7. PIANC, Navigation in muddy areas, PIANC-Bull. No 43, Rep. of Working Group No 3-a, 1982-1983, pp. 21-28.
8. van Bochove,P., Nederlof,L., Vaargedrag van diepstekende schepen in slibrijke gebieden, De Ingenieur, Jaarg. 91, No 30/31, 1979, pp. 525-530.
9. Kerckaert,P., Malherbe,B., Bastin,A., Navigation in muddy areas - The Zeebrugge experience, PIANC Bull. No 48, 1985, pp. 127-135.
10. Kerckaert,P., Vandenbossche,D., Malherbe,B., Druyts,M., Van Craenenbroeck,K., Maintenance dredging at the port of Zeebrugge : procedures to achieve an operational determination of the nautical bottom, Harbour Congress, V.II, KVIV, Antwerp, 1988, p. 4.13.
11. De Meyer,C., Malherbe,B., Optimization of maintenance dredging operations in maritime and estuarine areas, "Ports and Waterways", Buenos Aires, 1986.
12. Malherbe,B., The determination of the nautical bottom in muddy areas, Marintec, Shanghai, December 1985.
13. Malherbe,B., Nautical bottom research and survey for optimization of maintenance dredging in mud areas, Proc. Oceanology International, Brighton, 1986.
14. Wens,F., De Wolf,P., Vantorre,M., De Meyer,C. , A hydro-meteo system for monitoring shipping traffic in narrow channels in relation with the problem of the nautical bottom in muddy areas, 27th Int. Navigation Congress, S.II-1, PIANC, Osaka, 1990, pp. 5-16.
15. Vantorre,M., Coen,I., On sinkage and trim of vessels navigating above a mud layer, Proc. 9th Intern. Harbour Congress, V.II, KVIV, Antwerp, 1988, pp. 4.149-161.
16. Wehausen,J., Laitone,E., Surface waves, Encycopedia of Physics, band 9, Springer-Verlag, 1960.

APPENDIX

In a viscid Newtonian fluid, with mass density ρ and kinematic viscosity coefficient ν, the Navier-Stokes equations are

$$u\frac{\partial u}{\partial x} + w\frac{\partial u}{\partial z} = -\frac{1}{\rho}\frac{\partial p}{\partial x} + \nu\left(\frac{\partial^2 u}{\partial x^2} + \frac{\partial^2 u}{\partial z^2}\right) \qquad (A.1)$$

$$u\frac{\partial w}{\partial x} + w\frac{\partial w}{\partial z} = -\frac{1}{\rho}\frac{\partial p}{\partial x} + \nu\left(\frac{\partial^2 w}{\partial x^2} + \frac{\partial^2 w}{\partial z^2}\right) - g \qquad (A.2)$$

where p is the total pressure.

Multiplying both membes of the first and the second equation by u and w respectively, and summing up, lead to

$$\frac{D}{Dt}\left(p + \frac{1}{2}\rho V^2 + \rho g z\right) = \mu\left[u\left(\frac{\partial^2 u}{\partial x^2} + \frac{\partial^2 u}{\partial z^2}\right) + w\left(\frac{\partial^2 w}{\partial x^2} + \frac{\partial^2 w}{\partial z^2}\right)\right] \qquad (A.3)$$

(μ = dynamic viscosity, $V = (u^2 + w^2)^{1/2}$ = fluid velocity)

(A.3) leads to the Bernoulli equation if the fluid is inviscid.

ζ is the interface rise (positive upwards) with respect to its undisturbed horizontal level. We assume that in the very near vicinity of the fluid 1 - fluid 2 interface a laminar boundary sublayer exists, where the velocity gradient, thus also the gradient of u and w with respect to z, is linear, or $\partial^2 u/\partial z^2 = \partial^2 w/\partial z^2 = 0$ along this interface. Writing the remaining part between brackets of the viscosity term in (A.3), $u\,\partial^2 u/\partial x^2 + w\,\partial^2 w/\partial x^2$, in the form

$$u\frac{\partial}{\partial x}\left(\frac{\partial u}{\partial x}\right) + w\frac{\partial}{\partial z}\left(\frac{\partial u}{\partial x}\right) - w\frac{\partial}{\partial z}\left(\frac{\partial u}{\partial x}\right) + w\frac{\partial}{\partial x}\left(\frac{\partial w}{\partial x}\right)$$

reveals that in fact it is

$$u\frac{\partial}{\partial x}\left(\frac{\partial u}{\partial x}\right) + w\frac{\partial}{\partial z}\left(\frac{\partial u}{\partial x}\right) = \frac{D}{Dt}\left(\frac{\partial u}{\partial x}\right)$$

because $\partial w/\partial x - \partial u/\partial z = 0$, assuming irrotationality of the flow. Hence, (A.3) leads to

$$p + \frac{1}{2}\rho V^2 + \rho g z - \mu\frac{\partial u}{\partial x} = \text{constant} \qquad (A.4)$$

along the interface, i.e. on both sides, in fluid 1 and 2,

$$p_{d_A} + \frac{1}{2}\rho_1 V_1^2 - \mu_1\frac{\partial u_1}{\partial x} = p_{d_A} + \frac{1}{2}\rho_1 U^2 \qquad (A.5)$$

$$p_{d_A} + \frac{1}{2}\rho_2 V_2^2 + g(\rho_2 - \rho_1)\zeta - \mu_2\frac{\partial u_2}{\partial x} = p_{d_A} + \frac{1}{2}\rho_2 U^2 \qquad (A.6)$$

where p_d is the dynamic pressure being equal in adjacent points on each side of the interface, (point A fore of ship).

As along the interface line

$$V^2 = u^2\left[1 + \left(\frac{\partial\zeta}{\partial x}\right)^2\right] \tag{A.7}$$

u may be substituted for V in (A.5) and (A.6), if $\partial\zeta/\partial x$ is neglected. Hence, from (A.5) and (A.6),

$$\frac{1}{2}\rho_2 u_2^2 - \frac{1}{2}\rho_1 u_1^2 + g(\rho_2 - \rho_1)\zeta + \left(\mu_1\frac{\partial u_1}{\partial x} - \mu_2\frac{\partial u_2}{\partial x}\right) = \frac{1}{2}(\rho_2 - \rho_1)U^2 \tag{A.8}$$

along the interface. In inviscid fluid, (A.8) reduces to (3).

If $|\partial\zeta/\partial x| >> 0$, then

$$\frac{1}{2}\rho_2 u_2^2\left[1 + \left(\frac{\partial\zeta}{\partial x}\right)^2\right] - \frac{1}{2}\rho_1 u_1^2\left[1 + \left(\frac{\partial\zeta}{\partial x}\right)^2\right] + g(\rho_2 - \rho_1)\zeta + \left(\mu_1\frac{\partial u_1}{\partial x} - \mu_2\frac{\partial u_2}{\partial x}\right) = \frac{1}{2}(\rho_2 - \rho_1)U^2 \tag{A.9}$$

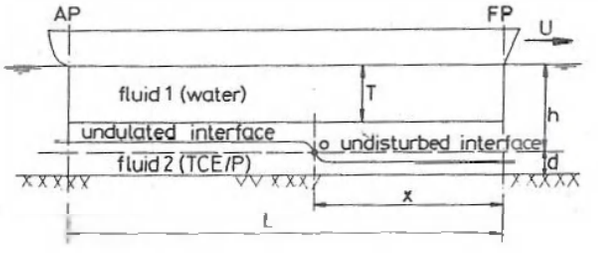

Fig. 1 : Schematic picture of longitudinal profile of interface alongside ship

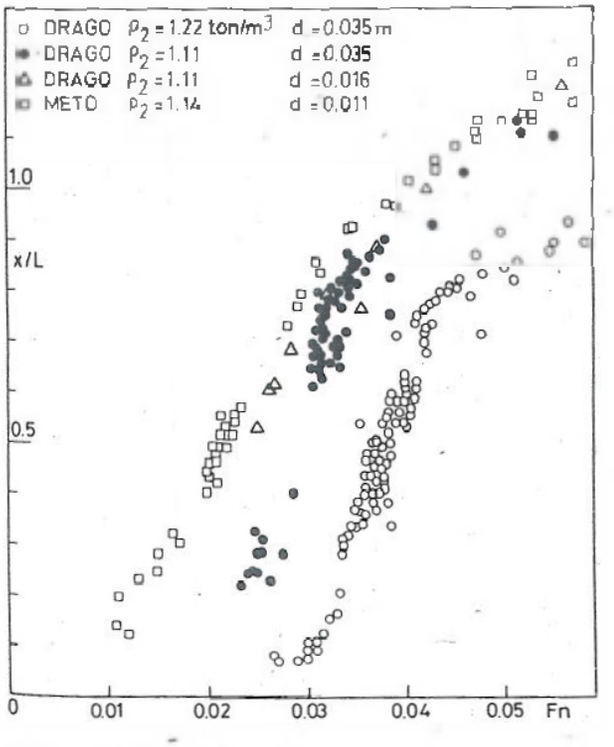

Fig.2 : Experimental values x/L

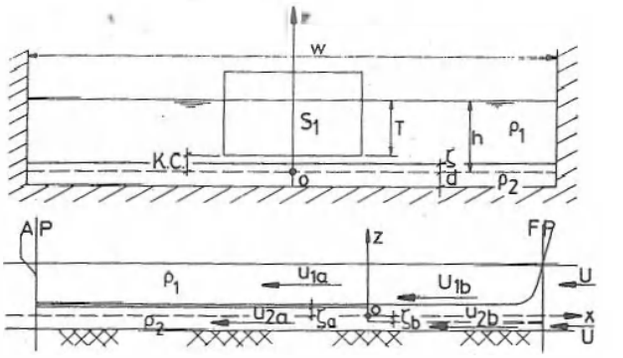

Fig.3 : Shipmodel tank and picture of flow

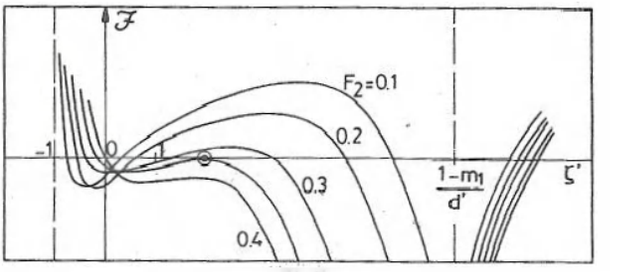

Fig.4 : Function F

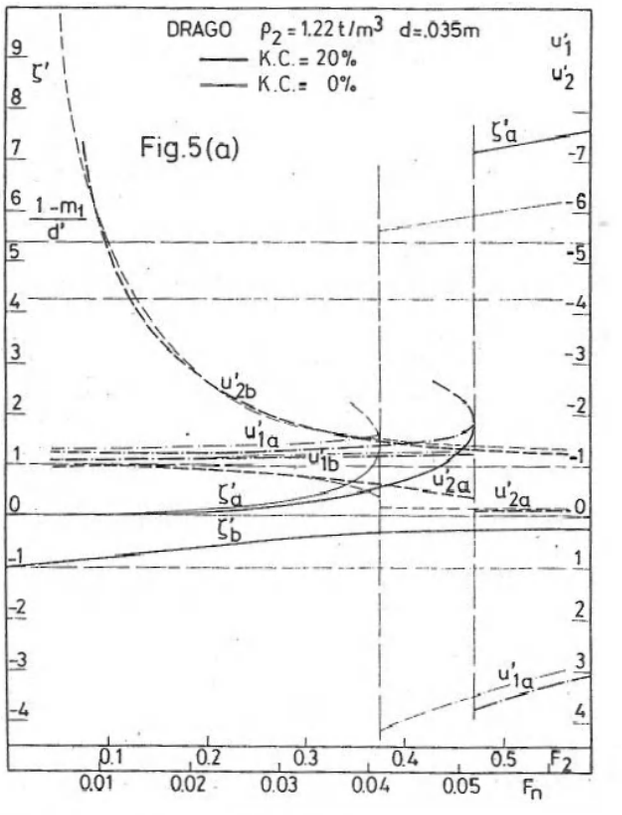

Fig.5 : Interface levels and fluid velocities in the layers

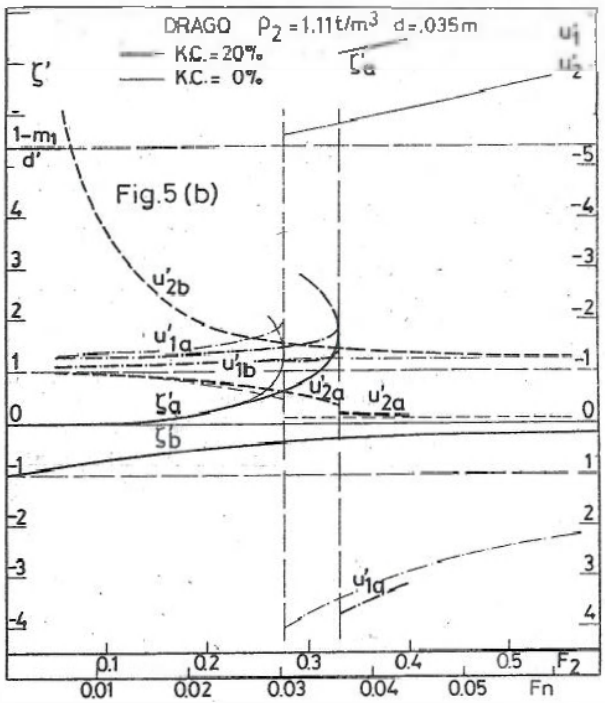

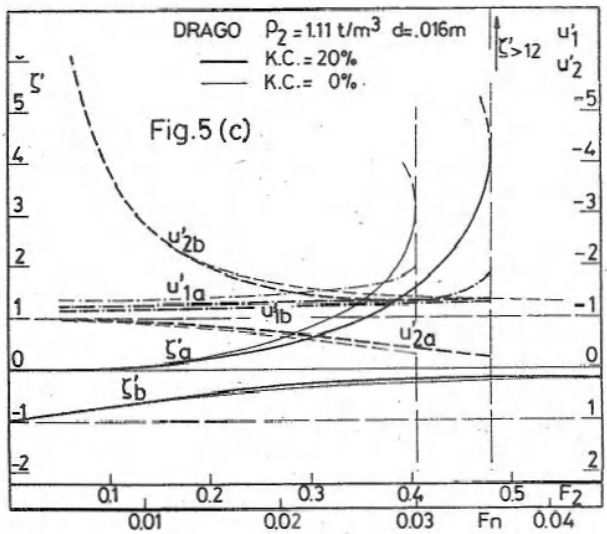

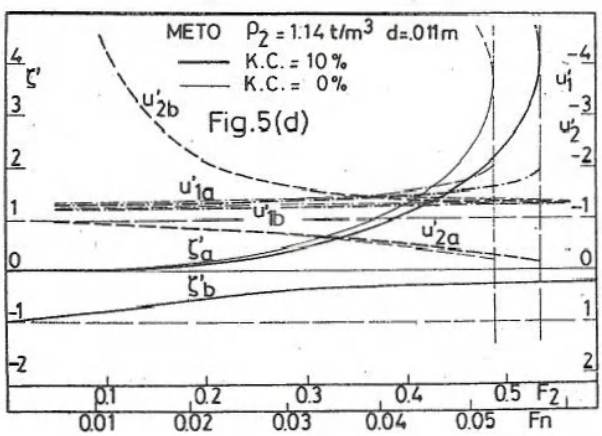

Fig. 5

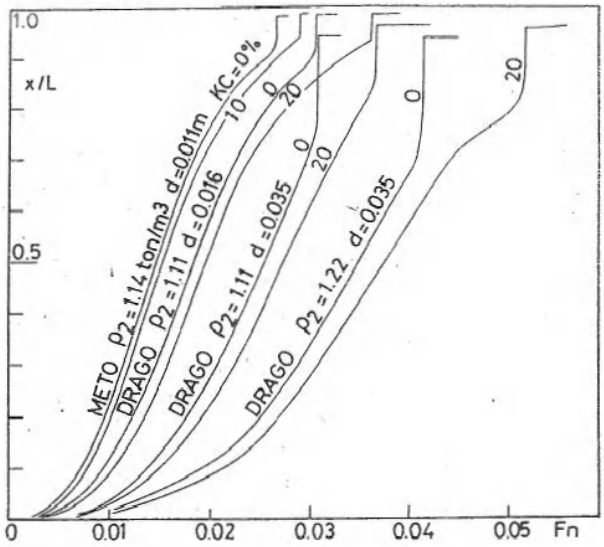

Fig.6 : Theoretical values x/L

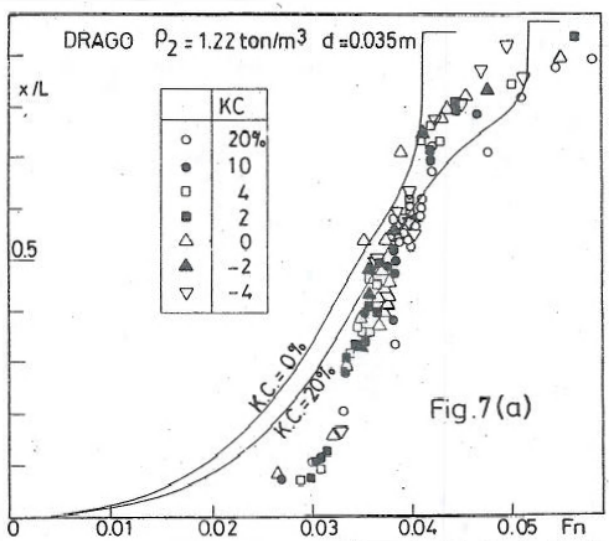

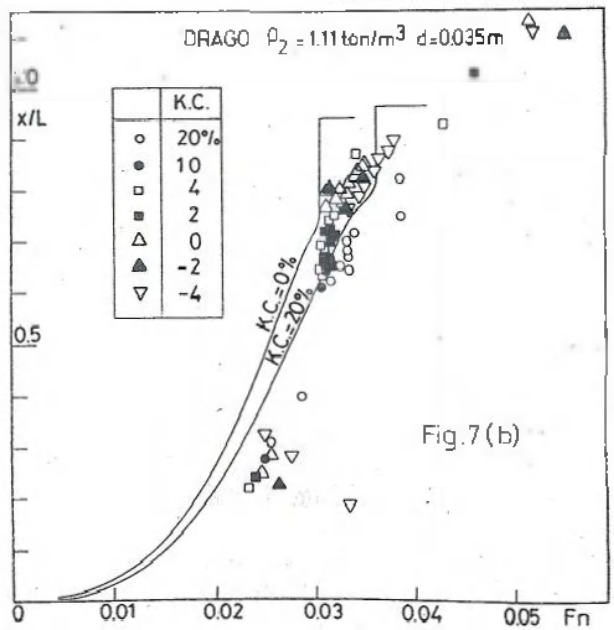

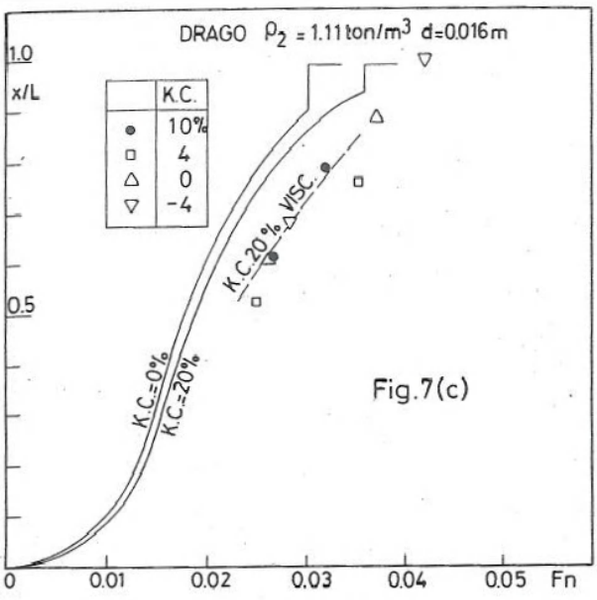

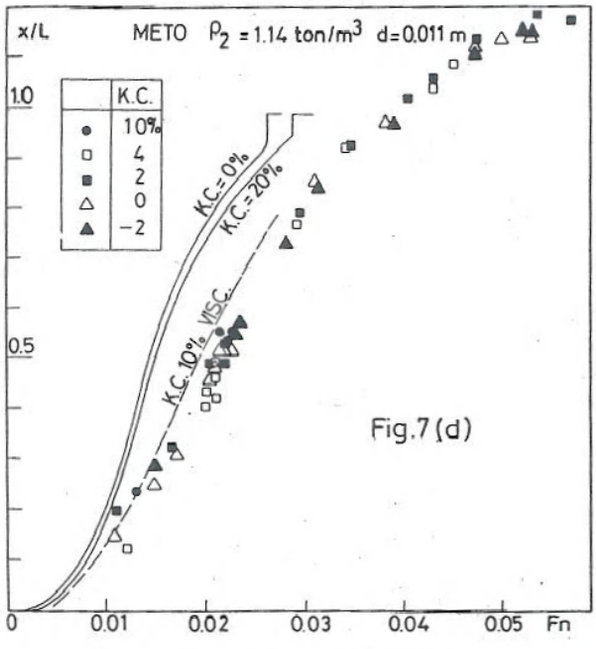

Fig.7 : Comparison theoretical and experimental values x/L

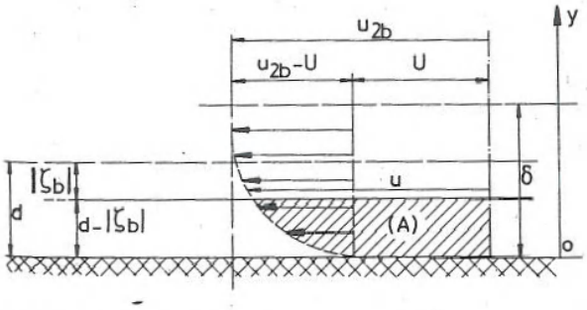

Fig.8 : Laminar boundary layer

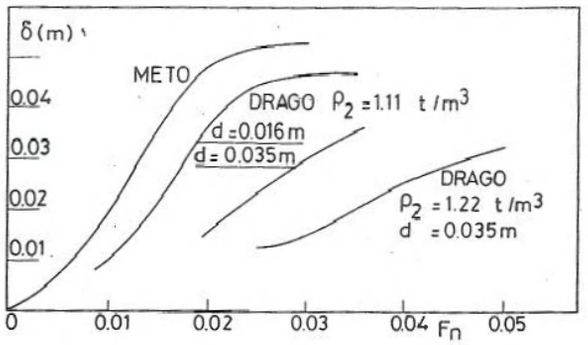

Fig.9 : δ at the jump

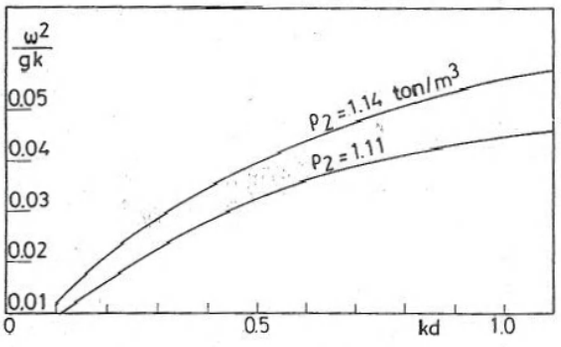

Fig.10 : Relation parameters interfacial waves

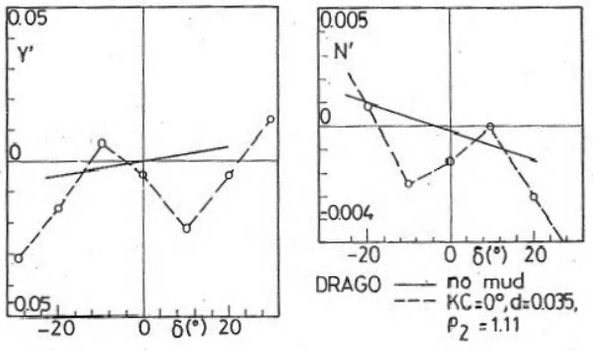

Fig.12 : Lateral force and yawing moment

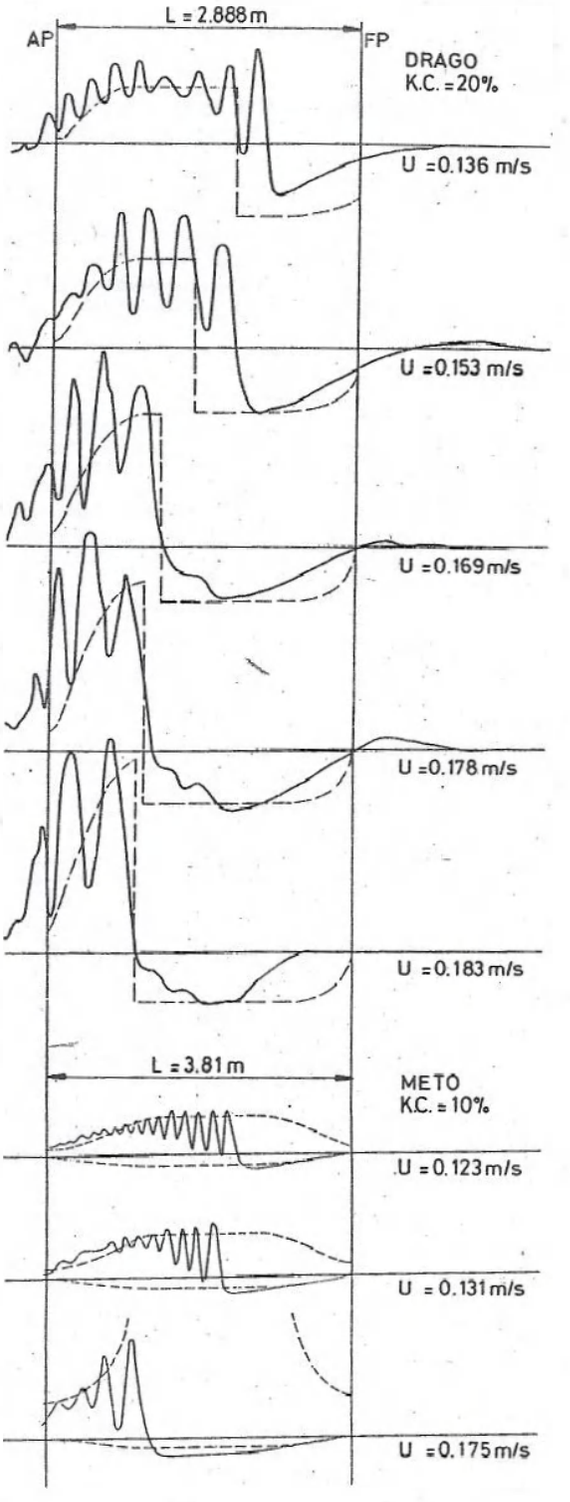

Fig.11 : Interface profiles